Synthesis of Nanostructured MnNiAPSO-34 Catalyst: Catalytic Properties and Performance

P. Sadeghpour[a, b], M. Haghighi[a, b,*]

[a] *Chemical Engineering Faculty, Sahand University of Technology, Sahand New Town, Tabriz, Iran.*
[b] *Reactor and Catalysis Research Center (RCRC), Sahand University of Technology, Sahand New Town, Tabriz,Iran.*

ARTICLE INFO

Article history:

Received 24 Jan. 2014
Accepted 17 Feb. 2014
Available online 15 May 2014

Keywords:

MnNiAPSO-34
Biomethanol
Ethylene
Propylene
MTO

ABSTRACT

Silicoaluminophosphate (SAPO-34) molecular sieve doped with transition metals, Mn and Ni, with different molar ratios (Mn/Ni=0.33, 3) was investigated for its activity, selectivity and lifetime in biomethanol to olefins reaction. MnNiAPSO-34 nanostructured catalyst was synthesized by hydrothermal method. Addition of metals was carried out by isomorphous substitution into the crystalline framework of SAPO-34. The nanostructured catalysts were characterized by XRD, FESEM, PSD, EDX, BET and FTIR techniques. MnNiAPSO-34 nanostructured catalyst synthesized with high concentration of Mn demonstrated larger crystallite size evidenced by XRD analysis. The FESEM results indicated that the concentration of metal ions could affect the morphology of nanostructured MnNiAPSO-34 catalyst due to different rate of crystal growth. The catalytic performance of the samples was studied in biomethanol to olefins reaction at atmospheric pressure and GHSV of 4200 $cm^3/g.h^{-1}$ in a fixed bed reactor. MnNiAPSO-34 with high concentration of Mn illustrated higher selectivity toward light olefins (60% after 180 min time on stream) and had longer lifetime.

1. Introduction

Ethylene and Propylene are important components in petrochemical industries with an increasing demand for their production [1, 2]. A remarkable array of light olefins applications creates a sense of excitement among researchers to explore newly accepted processes like biomethanol to olefins [3-6]. Methanol can be produced from syngas obtained by natural gas reforming [7-9]. However, in recent years, with the shortage of natural resources and energy, as well as the soaring prices of crude oil, more attention has been paid to the process of biomethanol catalytic dehydration to light olefins as a green route compared to the traditional routes [10, 11]. As a renewable fuel source biomethanol is used to produce light olefins. This biofuel is derived from biomass sources [12-14]. Some advantages of the referred process include the reduction of CO_2 emission and moderated operational conditions [14].

Corresponding author:
E-mail address: haghighi@sut.ac.ir (Mohammad Haghighi).

Recently many researches have focused on the synthesis of small pore molecular sieves which can be used in the conversion of biomethanol to olefins [15-19]. Silicoaluminophosphate SAPO-34 has been reported to be the most promising catalyst giving maximum light olefins selectivity up to 80%. Relatively mild acidity, high thermal stability, pore size of 0.43-0.5 nm and 8-membered ring pores are some of the favourable characteristics of SAPO-34 molecular sieves in converting biomethanol to olefins process [4, 20-23]. The main problem with these catalysts in industrial processes is their short life due to coke formation. Aromatics and branched isomers are formed within the catalyst cages where they are irreversibly absorbed on acidic sites; therefore, the concentration of acid sites decreases [6, 20, 23]. Physicochemical and catalytic properties of SAPO-34 catalyst can be affected by many factors such as acidity, particle size, particle shape and presence of heteroatoms [4, 24].

Many efforts have been made in order to modify SAPO-34 to increase light olefins yield and lifetime. It has been reported that SAPO-34 with metal incorporated into the framework shows higher ethylene selectivity and lower methane formation [22, 25]. The incorporation of heteroatoms into SAPO materials can be achieved through incipient wetness impregnation, ion exchange or isomorphous substitution. Isomorphous substitution is of particular interest as the heteroatoms, such as transition metal ions, are substituted into framework sites through the direct addition of the metal source to the synthesis mixture [26-28]. The difference in acidity generated in the catalyst is the main factor of isomorphs substitution over other methods [25, 29]. For this way of metal substitution into the framework, they carry the generic names MeAPSO-34 molecular sieves. By using various metals like transition metals the catalyst acidity could be modified. The latter is performed through creating new acid sites and, consequently, increasing the catalyst lifetime [28]. When heteroatoms are substituted into the framework, only minor perturbations to the electronic structure are formed. As a result, a heteroatom will replace more readily the aluminium and Brønsted acid sites created in the SAPO pores.

So far, many studies have focused on the modification of SAPO-34 by individual metals [30-32]. The type and concentration of metal ions and the method of incorporated metals into the framework of SAPO-34 catalyst could be significant in promoting the lifetime and improving the catalyst performance [29, 33]. According to the reported researches, nickel-containing SAPO-34 exhibits high selectivity of ethylene, while MnAPSO-34 was found to have longer lifetime in comparison with unmodified SAPO-34 [31, 34-37]. Due to the importance of biomethanol to olefins process, various researches have been conducted to improve SAPO-34 properties. Therefore, investigation on synthesis of this catalyst could be effective in controlling catalyst structure and improving its properties.

The main objective of this paper is to develop doped SAPO-34 catalyst by introducing Mn and Ni metals for the biomethanol reaction to produce olefins. Nanostructured $Mn_{0.05}Ni_{0.15}$APSO-34 and $Mn_{0.15}Ni_{0.05}$APSO-34 catalysts with 0.05 and 0.15 metal oxide ratio in the initial gel were synthesized and compared. Physicochemical properties of these nanostructured catalysts were identified by XRD, FESEM, PSD, EDX, BET and FTIR techniques. The performance tests were carried out to investigate the effect of different temperatures on the nanostructured catalyst activity. The stability test was conducted to investigate the effect of time on stream.

2. Experimental

2. 1. Materials

In a typical hydrothermal synthesis, aluminium triisopropylate (Merck, 98%), fumed silica (Aldrich, 99.8%), phosphoric acid (Merck, 85%) and DEA (Aldrich, 99%) were used as the sources of aluminium, silicon, phosphorus and organic templates, respectively. Nickel nitrate hexahydrate (Merck) and manganese nitrate tetrahydrate (Merck) were used as the metal sources. Also, de-ionized water purchased from the Kasra Company was used to prepare the solutions. The synthesized

nanostructured catalysts with Mn to Ni metal oxide ratios in the initial gel equal to 0.05 and 0.15 were denoted as $Mn_{0.05}Ni_{0.15}$APSO-34 and $Mn_{0.15}Ni_{0.05}$APSO-34.

2. 2. Preparation and Procedures

Nanostructured catalysts were synthesized by a hydrothermal method using DEA as an organic agent. 10.90 g of aluminum triisopropylate and an amount of de-ionized water were dissolved in distilled water under stirring conditions for 1.5 h. Then, 6.03 g of Phosphoric acid aqueous solution was added by a drop-wise addition to the mixture under stirring for 0.5 h. After half an hour, 0.94 g of fumed silica was added into the solution and stirred for 30 min to achieve a uniform mixture. Next, a weighed amount of nickel nitrate hexahydrate and manganese nitrate tetrahydrate were added and the solution was stirred for 0.5 h after the addition of each solution. Finally, 3.86 g of diethyl amine as the template was added slowly. The chemical composition of the synthetic gel was as follows: $1Al_2O_3$: $0.6SiO_2$: $1P_2O_5$: 2DEA: xMnO: yNiO: $70H_2O$, where *x* and *y* represent the molar ratio of the nickel and manganese oxides in the initial gel, equal to 0.05, 0.15 and 0.15, 0.05 for $Mn_{0.05}Ni_{0.15}$APSO-34 and $Mn_{0.15}Ni_{0.05}$APSO-34, respectively. The resulted gel was transferred into an autoclave where it was heated at 200 ºC for 48 h. The solid product was recovered by filtration, washed several times with distilled water and dried at 110 ºC overnight. Finally, the nanostructured catalyst sample was calcined at 550 ºC for 12 h to remove the organic template and the water content trapped within the micro pores of the as-synthesized solid. A typical preparation procedure of $Mn_{0.05}Ni_{0.15}$APSO-34 and $Mn_{0.15}Ni_{0.05}$APSO-34 samples is shown in Fig. 1.

2. 3. Characterization Techniques

X-ray diffraction patterns (XRD) were recorded on a Bruker D8 Advance diffractometer with Cu Kα radiation (1.54178˚A) to identify the crystal phases in the range of 2θ = 8-50˚. The phase identification was done by comparison to the Joint Committee on Powder Diffraction Standards (JCPDSs). Morphology of the nanostructured catalyst was investigated using field emission scanning electron microscopy (FESEM), HITACHI S-4160. to improve conductivity, the samples were covered with a thin gold film (ion sputtering). Chemical composition of the nanostructured catalysts was determined by an SEM equipped with an energy dispersive X-ray (EDX- dot mapping) analyser, Scan MV 2300 Cam. Brunner-Emmett-Teller (BET) surface area was measured using nitrogen adsorption/desorption isotherms by a micrometric Quantachrome (Chambet 3000) analyzer. Infrared analysis of the nanostructured catalyst was carried out by a UNICAM 4600 FTIR spectroscopy addressing surface functional groups.

2. 4. Experimental Setup for Catalytic Performance Test

To produce the gas stream containing N_2, biomethanol and H_2O, a saturator was applied. The saturator container has an inlet pathway for the carrier gas N_2. To produce a reaction gas stream with the desired biomethanol concentration, N_2, composed of 10 mol% biomethanol and 90 mol% H_2O, entered the saturator with a constant flow rate of 70 ml/min. It was permitted to flow with a gaseous space velocity of 4200 $cm^3/gr.hr^{-1}$. The reaction was carried out in a U-shape Pyrex fixed bed reactor (internal diameter = 0.008m, length = 0.32 m) heated by a temperature controlled electric furnace. The reaction was conducted at atmospheric pressure. Experiments were performed using 1 g of the nanostructured catalyst at the temperature range 300-500 ºC. Reactions were conducted in order to study the effect of reaction temperature on the nanostructured catalyst activity. The gas compositions of the reactants and products were analysed using a gas chromatograph (GC Chrom, Teif Gostar Faraz, Iran) equipped with Plot-Q columns and FID detectors. Gas stream from the regulators passed through pipes and was introduced to the mass flow controllers (MFC). The gases were mixed and passed to the reaction section. Argon was used as the carrier gas for gas chromatography and hydrogen was used to regenerate the nanostructured catalyst prior to the experiments. To ensure reproducibility of the results, the experiments were repeated several

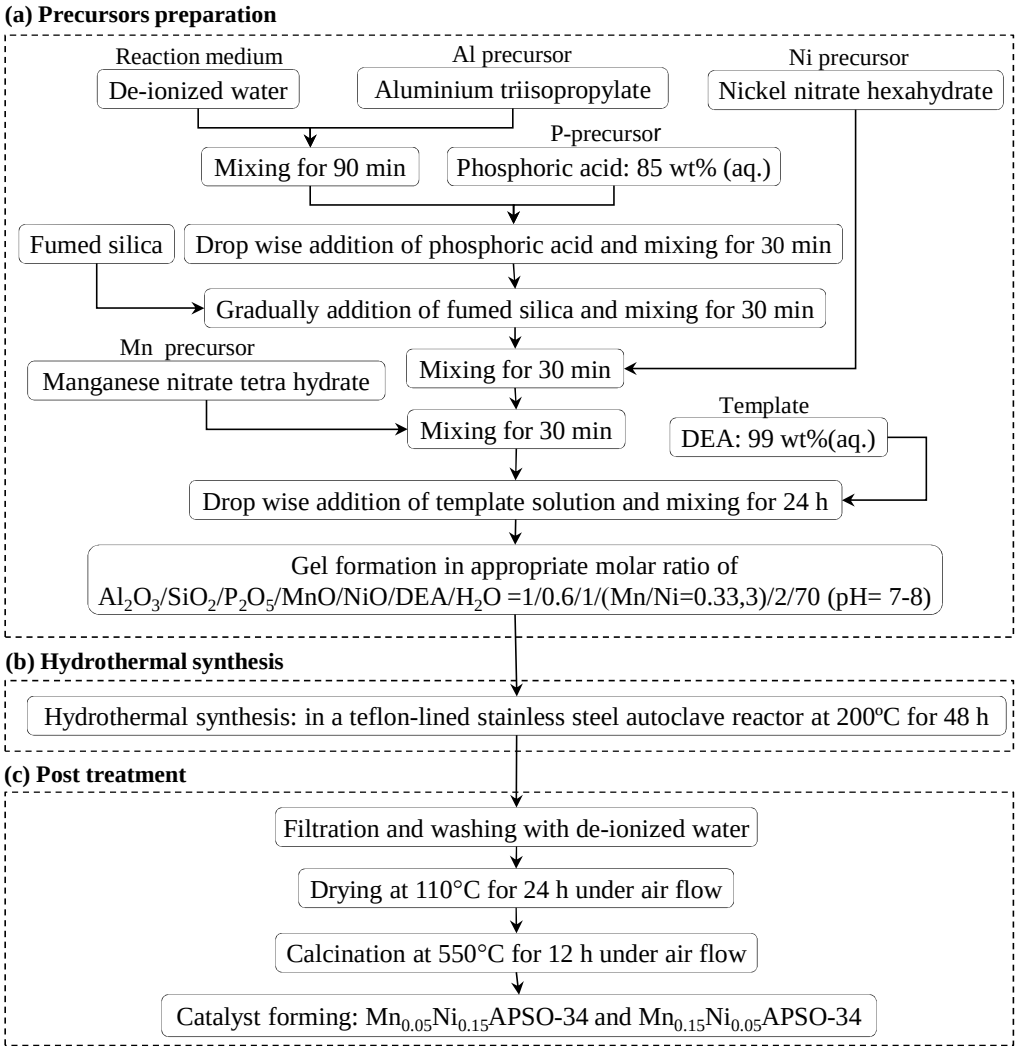

Fig. 1. Preparation steps of nanostructured $Mn_{0.05}Ni_{0.15}$APSO-34 and $Mn_{0.15}Ni_{0.05}$APSO-34 catalysts

times under similar conditions.

3. Results and Discussion

3. 1. Physicochemical Characterizations

3. 1. 1. XRD Analysis

X-ray diffraction patterns of the synthesized MnNiAPSO-34 samples prepared by Mn and Ni modifiers with different concentrations are shown in Fig. 2. A detailed examination of these patterns reveals the formation of SAPO-34 rhombohedra structure (JCPDS: 01-087-1527), indicating high crystallinity and purity of the samples by diffraction peak at 2θ = 9.5, 12.8, 20.6 and 31°, which is similar to those SAPO-34s reported in literature in the absence of any impurity for both nanostructured catalysts [30, 32, 33]. Moreover, it is evident that $Mn_{0.05}Ni_{0.15}$APSO-34 and $Mn_{0.15}Ni_{0.05}$APSO-34 could be successfully crystallized at different concentrations of heteroatoms in the initial gel mixture; however, no clear pattern corresponding to the metal oxides was observed in the XRD record of nanostructured catalysts due to low amount of Ni and Mn loading or high dispersion in the framework. This result is in good agreement with the previous studies [31].

Fig. 3 shows the relative crystallinity and average crystallite size of the nanostructured MnNiAPSO-34 catalysts prepared with different concentrations of Mn and Ni. The relative crystallinity of MnNiAPSO-34 catalysts was measured using the intensity of

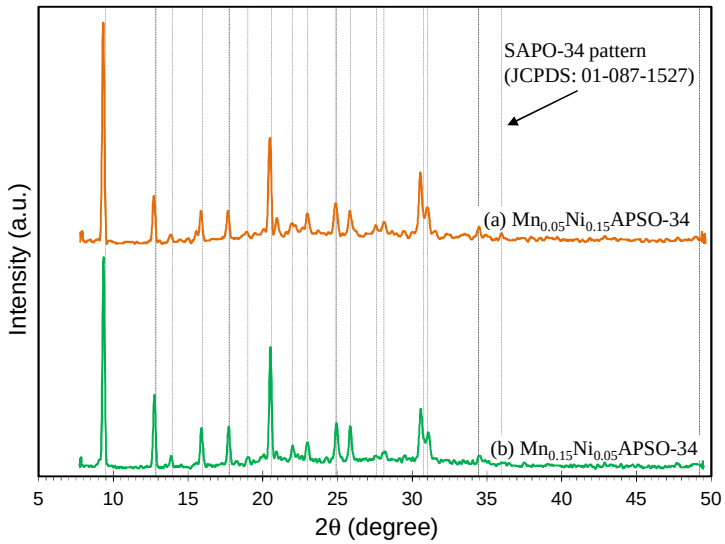

Fig. 2. XRD patterns of the synthesized nanostructured catalysts: (a) $Mn_{0.05}Ni_{0.15}$APSO-34 and (b) $Mn_{0.15}Ni_{0.05}$APSO-34

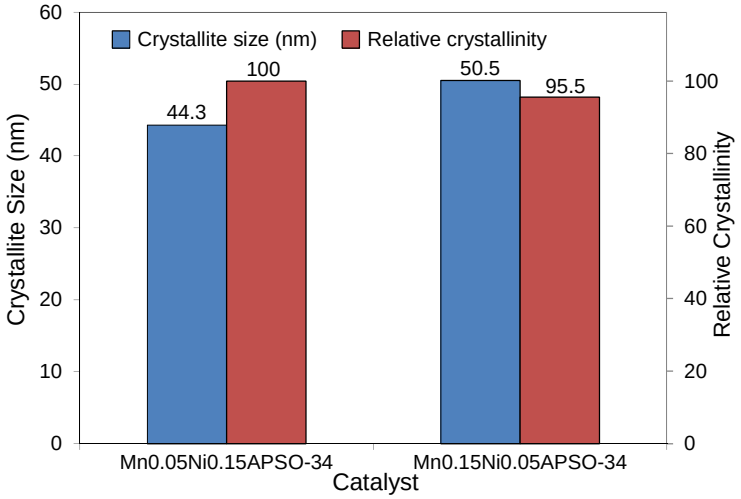

Fig. 3. Crystallite size and relative crystallinity of the nanostructured $Mn_{0.05}Ni_{0.15}$APSO-34 and $Mn_{0.15}Ni_{0.05}$APSO-34 catalysts

the most important peak at $2\theta = 9.5^{\circ}$ on the basis of the best prepared sample with highest crystallinity as the reference. The crystallite size was calculated using standard Debye-Scherrer equation. According to this figure, it is concluded that the concentration of metals has influential low effect on both nucleation and crystal growth rates. The diffraction peaks were very sharp. The relative crystallinity of the nanostructured $Mn_{0.05}Ni_{0.15}$APSO-34 and $Mn_{0.15}Ni_{0.05}$APSO-34 catalysts was found to be 100 and 95.5%, respectively. So, the crystallinity of $Mn_{0.15}Ni_{0.05}$APSO-34 nanostructured catalyst prepared by Mn/Ni=3 ratio is lower than that of the other sample. This means that the distribution of higher Ni concentration in SAPO framework increased the number of crystal nuclei. As the dimensions of the obtained nanostructured catalysts confirmed, the average crystal size of these nanostructured catalysts was about 44.3 and 50.5 nm. It seems that increasing the Mn contents of the sample leads to rapid crystal growth rates yielding crystals of larger size with fewer defects.

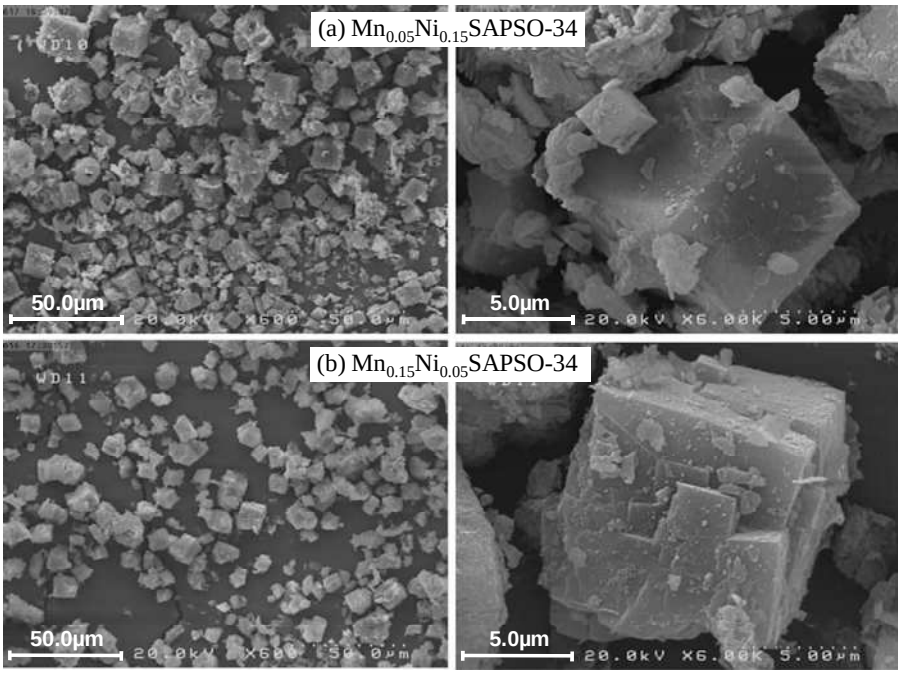

Fig. 4. FESEM images of the synthesized nanostructured catalysts: (a) $Mn_{0.05}Ni_{0.15}$APSO-34 and (b) $Mn_{0.15}Ni_{0.05}$APSO-34

3. 1. 2. FESEM Analysis

Fig. 4 illustrates FESEM images of (a) $Mn_{0.05}Ni_{0.15}$APSO-34 and (b) $Mn_{0.15}Ni_{0.05}$APSO-34 nanostructured catalysts prepared with different concentrations of modifiers. As can be seen, the catalyst particles have similar cubic morphology like natural Chabazite with an obvious small aggregation differing in particle size. The difference in the particle sizes comes from different metal loadings and due to the presence of small particles on the $Mn_{0.05}Ni_{0.15}$APSO-34 and $Mn_{0.15}Ni_{0.05}$APSO-34 particles surface can be attributed to the manganese and nickel modifiers. The particle size of $Mn_{0.15}Ni_{0.05}$APSO-34 sample was greater than that of $Mn_{0.05}Ni_{0.15}$APSO-34 sample. The FESEM study confirms that morphology of the final product depends on the gel composition used in the synthesis. Furthermore, the nanostructured catalyst containing molar ratio Mn/Ni=0.33 resulted in the formation of particles with smoother external surface. The obtained results from FESEM images are in good consistency with the corresponding XRD analysis in which $Mn_{0.15}Ni_{0.05}$APSO-34 sample exhibits less intense and broader peaks. This consistency between XRD and FESEM can be explained based on the fact that crystallization rates for the two catalysts were different because of the incorporation of different concentration of Mn and Ni metal ions and the crystal growth around the large number of nuclei created the smaller particles.

3. 1. 3. PDS Analysis

Fig. 5 shows the particle size distribution (PSD) of the synthesized nanostructured catalysts for $Mn_{0.05}Ni_{0.15}$APSO-34 (a) and $Mn_{0.15}Ni_{0.05}$APSO-34 (b). As indicated in the figure, for the nanostructured $Mn_{0.05}Ni_{0.15}$APSO-34 catalyst, 52% of particles size is in the range of 5-10 µm. Furthermore, the particle size is between 3.4-20.5 µm with an average size of 7.4 µm. However, the particle size is in the range of 4.9-20.1 µm for the sample synthesized with high concentration of Mn ($Mn_{0.15}Ni_{0.05}$APSO-34). More uniform particle size distribution is achieved by applying molar ratio of Mn/Ni=3 as a result of which 68.4% of particles are in the range of 5-10 µm with an average size of 9.1 µm. So, large grains of nanostructured $Mn_{0.15}Ni_{0.05}$APSO-34 catalyst are formed using high concentration of Mn owning particles of about 9.1 µm.

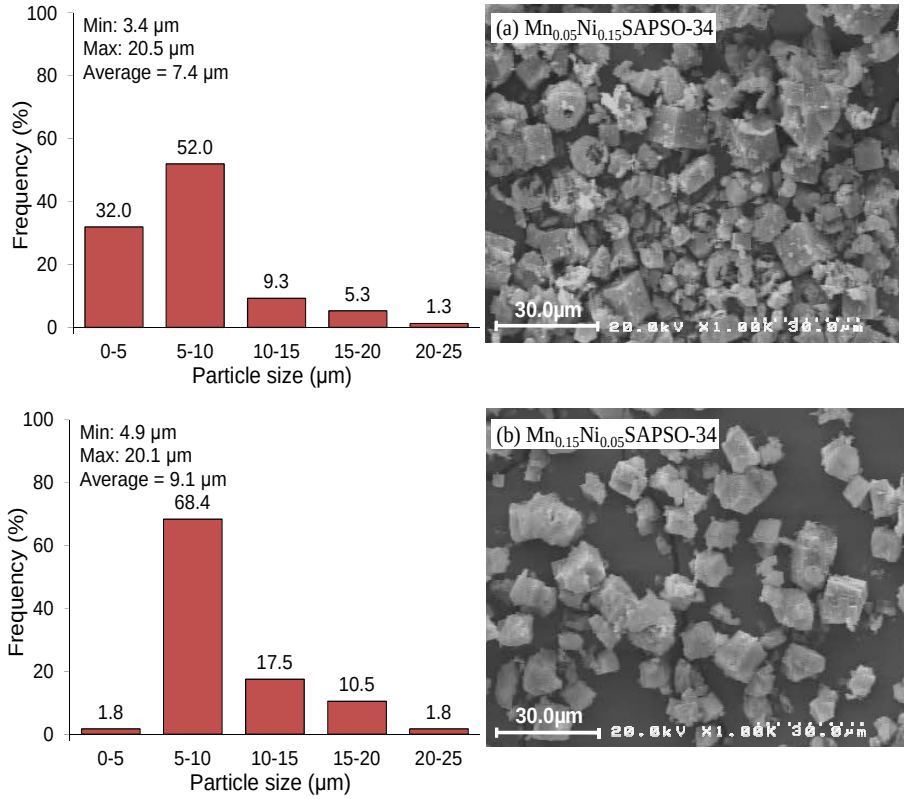

Fig. 5. Particle size histogram of the synthesized nanostructured catalysts: (a) $Mn_{0.05}Ni_{0.15}$APSO-34 and (b) $Mn_{0.15}Ni_{0.05}$APSO-34

3. 1. 4. EDX Analysis

Fig. shows the EDX dot-mapping micrographs for $Mn_{0.05}Ni_{0.15}$APSO-34 and $Mn_{0.15}Ni_{0.05}$APSO-34 nanostructured catalysts. All the materials used in the preparation of MnNiAPSO-34 catalysts (Si, Al, P, Mn and Ni), some of which were not detected in the XRD, could be observed in the EDX dot-mapping analysis. The EDX dot-mapping micrographs show high dispersion and uniform morphology for Ni in $Mn_{0.05}Ni_{0.15}$APSO-34 and high dispersion of Mn in $Mn_{0.15}Ni_{0.05}$APSO-34 sample. After removal of the template during the calcination in synthesized catalysts with appropriate distribution of metals in the framework of SAPO-34 and formation of the Brønsted acid sites inside the pores, new acid sites significantly improve the catalytic performance with proper distribution of Si in crystal lattice structures. Furthermore, according to the obtained results, during the synthesis and maintenance of the synthetic samples no impurities were observed.

Fig. shows the gel vs. crystal composition of the synthesized nanostructured catalysts for (a) $Mn_{0.05}Ni_{0.15}$APSO-34 and (b) $Mn_{0.15}Ni_{0.05}$APSO-34. This analysis was applied locally indicating that the molar percentages to the total catalyst have little credibility. However, distribution of molar percentages in the products is consistent with the results of EDX analysis for the synthetic gel. Comparing with the Si content of the starting gels (11 mol%), the Si content of $Mn_{0.15}Ni_{0.05}$APSO-34 was higher than $Mn_{0.05}Ni_{0.15}$APSO-34 catalyst; this means that more amounts of Si is incorporated into the framework of modified nanostructured catalyst with molar ratio of Mn/Ni=3 and/or they remain as amorphous silica on extra framework. According to the acceptable crystallinity observed from the XRD data, it is evident that the presence of silica as the amorphous phase is unreasonable. The molar percentages of Ni modifier in the gel structure and final product in the $Mn_{0.05}Ni_{0.15}$APSO-34 catalyst are higher than those in the $Mn_{0.15}Ni_{0.05}$APSO-34 sample synthesized with low concentration of Ni.

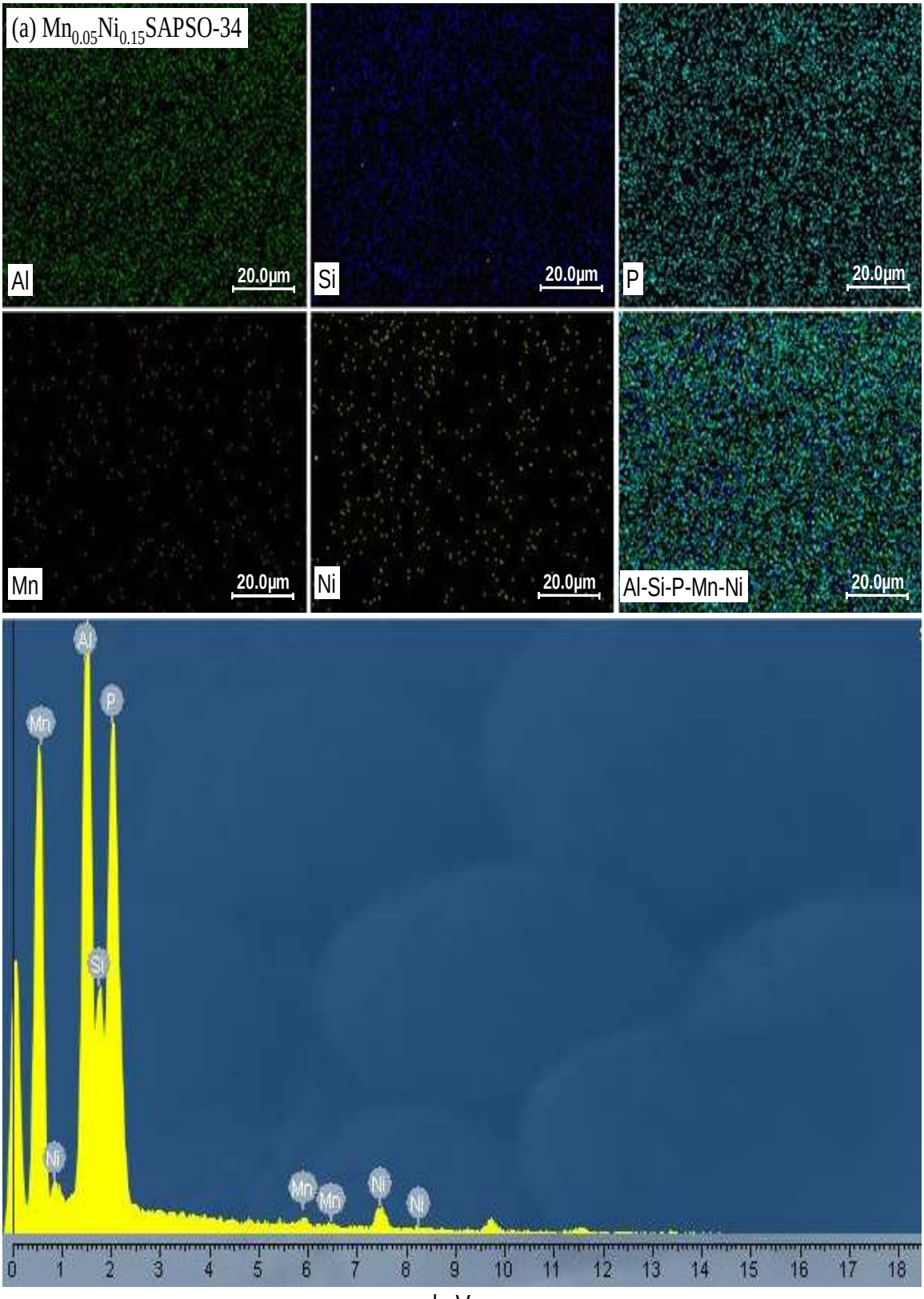

Fig. 6. EDX analysis of the synthesized nanostructured catalysts: (a) $Mn_{0.05}Ni_{0.15}$APSO-34

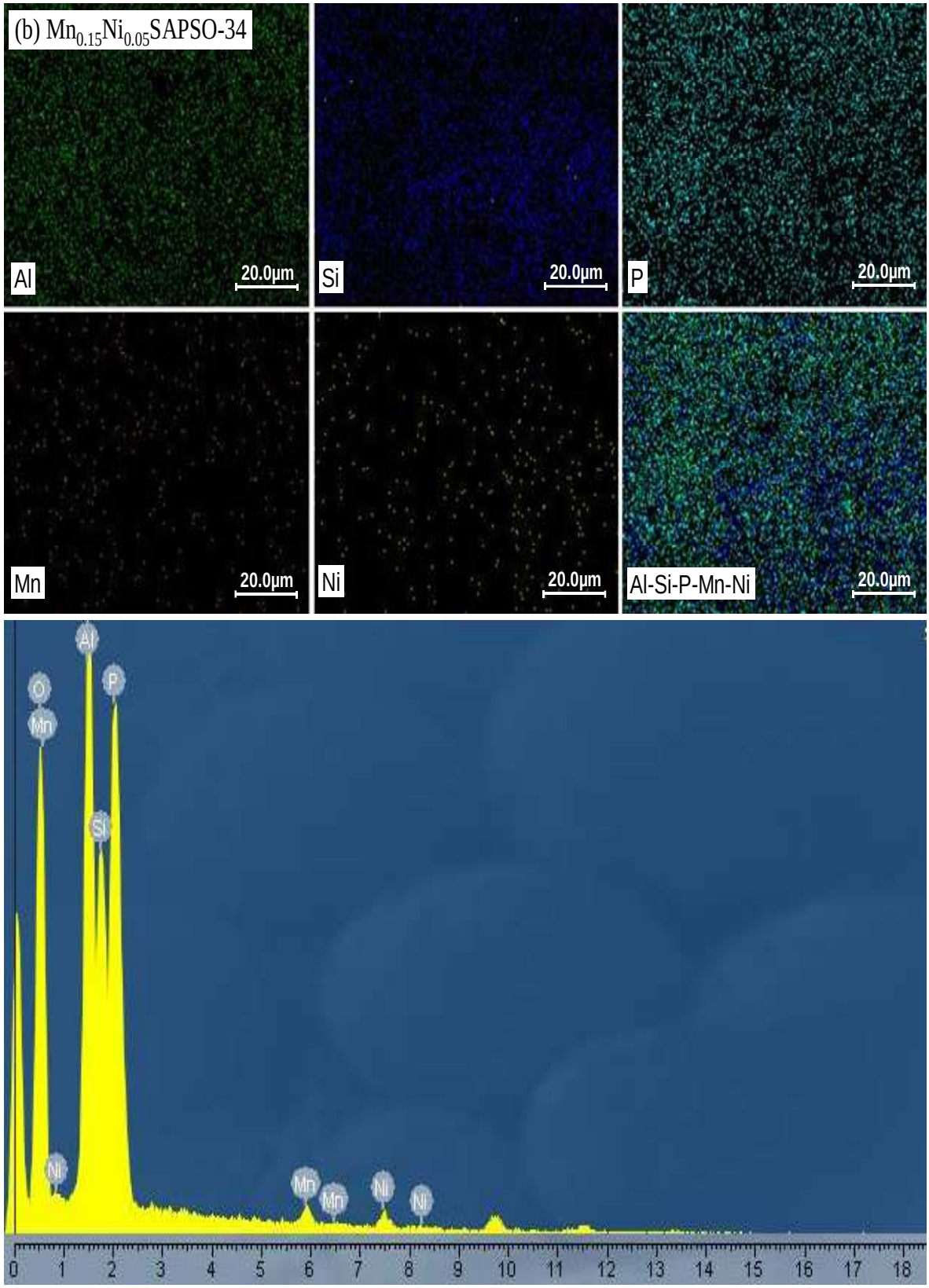

Fig. 6. EDX analysis of the synthesized nanostructured catalysts: (b) $Mn_{0.15}Ni_{0.05}$APSO-34

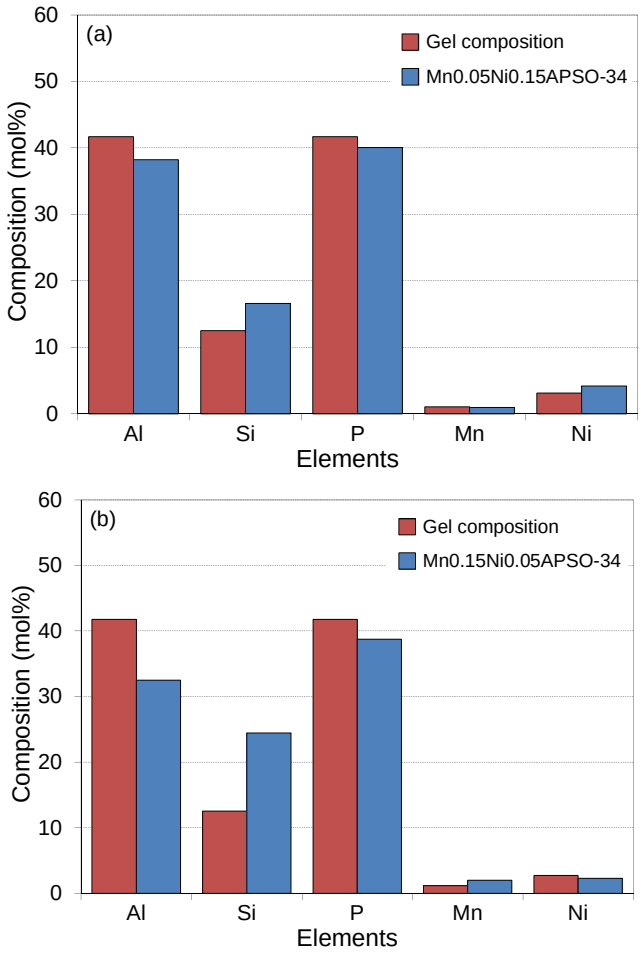

Fig. 7. Gel vs. crystal composition of the synthesized nanostructured catalysts: (a) $Mn_{0.05}Ni_{0.15}$APSO-34 and (b) $Mn_{0.15}Ni_{0.05}$APSO-34

3. 1. 5. BET Analysis

The BET surface areas possessed areas about 434.0 and 303.2 m^2/g for $Mn_{0.05}Ni_{0.15}$APSO-34 and $Mn_{0.15}Ni_{0.05}$APSO-34 nanostructured catalysts, respectively. It describes that the BET surface area decreased by addition of high concentration of Mn modifier. High surface area is an indication of a higher degree of crystallinity by x-ray diffraction and small particle sizes observed by scanning electron microscopy techniques. The difference in the ability between framework and extra-framework metals in the catalysts framework could be a reason for the discrepancy in the surface areas.

3. 1. 6. FTIR Analysis

The series of materials corresponding to CHA structure were characterized by FTIR technique as shown in Fig. . To achieve a more precise IR characterization, spectra were reported in a wide range of frequency 500-4000 cm^{-1}. The spectra of the synthesized nanostructured catalysts showed peaks of stretching vibration of structural O-H for Si(OH)Al bridging hydroxyl group at 3450 cm^{-1} [38-40]. The stretching vibration around 1660 cm^{-1} can be attributed to the physically adsorbed water [41-43]. The peaks at wave numbers about 1100, 870, 630, and 480 cm^{-1} are assigned to the T-O-T symmetric stretching, protonated template, T-O bending in D-6 rings and T-O bending of Si tetrahedral exhibiting characteristic peaks of SAPO-34 phase, respectively. The change of D-6 ring peaks intensity corresponding to the CHA framework would be the key evidence for a successful synthesis of SAPO-34 in the samples. The hydroxyl groups are active sites. No more

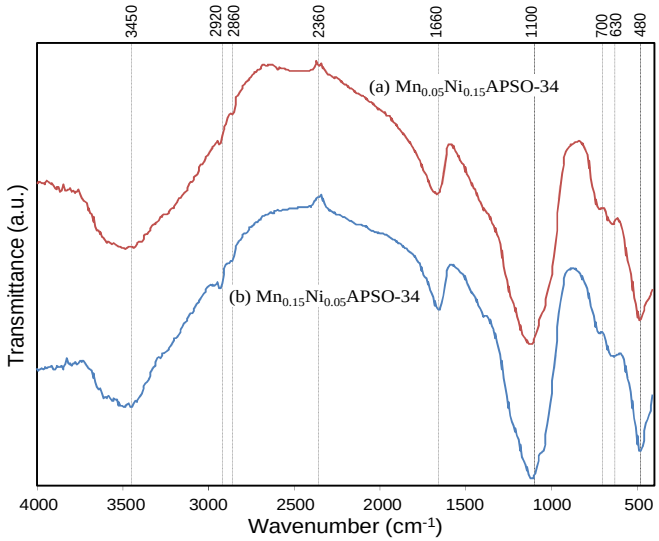

Fig. 8. FTIR spectra of the synthesized nanostructured catalysts: (a) $Mn_{0.05}Ni_{0.15}$APSO-34 and (b) $Mn_{0.15}Ni_{0.05}$APSO-34.

considerable increase in the concentration of strong acidic hydroxyl groups, corresponding to the varying concentration of Mn and Ni modifiers is observed.

3. 2. Catalytic Performance Study toward MTO Reaction

3. 2. 1. The Effect of Nanostructured Catalyst on Biomethanol Conversion

The catalytic activity of nanostructured catalysts in terms of reactant conversion and product selectivity was studied at temperatures ranging from 300 to 500°C. In this section, all reactions were carried out at a constant molar feed ratio and gas hourly space velocity. It should be noted that the nanostructured catalyst was dehydrated by Argon flow before the reaction. A typical material balance was carried out for some of the experiments and it was found that the value is acceptable (±3% error). The difference in the concentration of metal ions may affect the activity and product distribution. So, Fig. presents the biomethanol conversion in biomethanol to olefins reaction on MnNiAPSO-34 samples with different Mn and Ni contents. The conversion of biomethanol was defined as the percentage of biomethanol consumed for its production during this reaction. The main goal of biomethanol conversion is to obtain higher selectivity of C_2-C_4 olefins. According to the figure, at 300 ºC, the nanostructured catalysts activity is low which is enhanced by increasing temperature up to 500 ºC. It can be concluded that the concentration of metals has influential low effect on biomethanol conversion.

3. 2. 2. Effect of Nanostructured Catalyst on Product Selectivity

The distribution of products over $Mn_{0.05}Ni_{0.15}$APSO-34 and $Mn_{0.15}Ni_{0.05}$APSO-34 nanostructured catalysts at 300-500 ºC is illustrated in Fig. . As the temperature increases from 300 to 500°C, the C_3H_6 selectivity decreases which can be as a result of simultaneous occurrence of methane formation and propylene conversion to ethylene reactions at higher temperatures. Therefore, in the two nanostructured catalysts, the production of ethylene increased gradually with increasing of temperature to 400 ºC, and decreased afterward. The $Mn_{0.15}Ni_{0.05}$APSO-34 nanostructured catalyst produced a higher ethylene in comparison with the $Mn_{0.05}Ni_{0.15}$APSO-34 sample. Distribution of Mn and Ni metal ions with different concentrations has a little effect on selectivity towards propylene.

Methane is an undesirable product for olefins production. The possible reaction mechanism of methane formation at high temperatures is defined as follows [44]:

$2\ CH_3OH \rightarrow CH_3OCH_3 + H_2O$ [1]

$CH_3OCH_3 + H_2O \rightarrow 2CO + 4H_2$ [2]

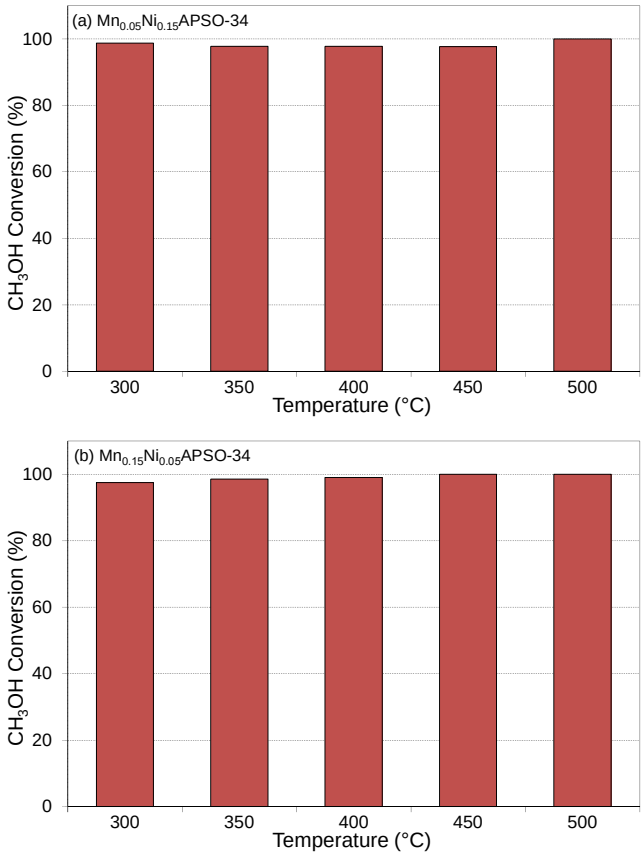

Fig. 9. Biomethanol conversion over the synthesized nanostructured catalysts: (a) $Mn_{0.05}Ni_{0.15}$APSO-34 and (b) $Mn_{0.15}Ni_{0.05}$APSO-34

$$2CO + 2H_2 \rightarrow CO_2 + CH_4 \quad [3]$$

Increasing temperature causes the formation of CH_4 by-products which leads to the reduction of light olefins percentage in the product stream. This occurs due to the thermal decomposition of DME into methane and carbon dioxide at high temperatures [44-46]. The amount of CH_4 formation in the $Mn_{0.05}Ni_{0.15}$APSO-34 nanostructured catalyst is higher than that in the $Mn_{0.15}Ni_{0.05}$APSO-34 sample synthesized with low concentration of Ni. After simultaneous consideration of the highest bio-CH_3OH conversion and light olefins selectivity for the nanostructured catalysts, the temperature value of 400°C was selected to investigate the effect of time on steam.

3. 2. 3. Effect of Time on Stream Performance

Fig. (a) shows the distribution of major products during time on stream (TOS) for the $Mn_{0.05}Ni_{0.15}$APSO-34 nanostructured catalyst at 400°C. For this sample, biomethanol conversion drops from 95 to 63% after 1 h TOS. The nanostructured catalysts lifetime is defined as the reaction time sustaining nanostructured catalyst activity until the selectivity of olefins is lower than 60%. The maximum ethylene selectivity was about 60%. Also, both the ethylene and the propylene in the product decreased to below than 1% at 5 h. The maximum C_2-C_4 olefins observed (80%) in the early hours of TOS steadily decreased with a concomitant increase in the selectivity of by-products such as DME. Weak acid sites are useless for olefins production, but biomethanol can be converted to DME on weak acid sites. Thus, after deactivation, when most of the strong and moderate acid sites were blocked by coke formation, the selectivity of light olefins decreased rapidly.

Fig. (b) shows the product distribution of $Mn_{0.15}Ni_{0.05}$APSO-34 at 400°C. $Mn_{0.15}Ni_{0.05}$APSO-34 reveals similar biomethanol

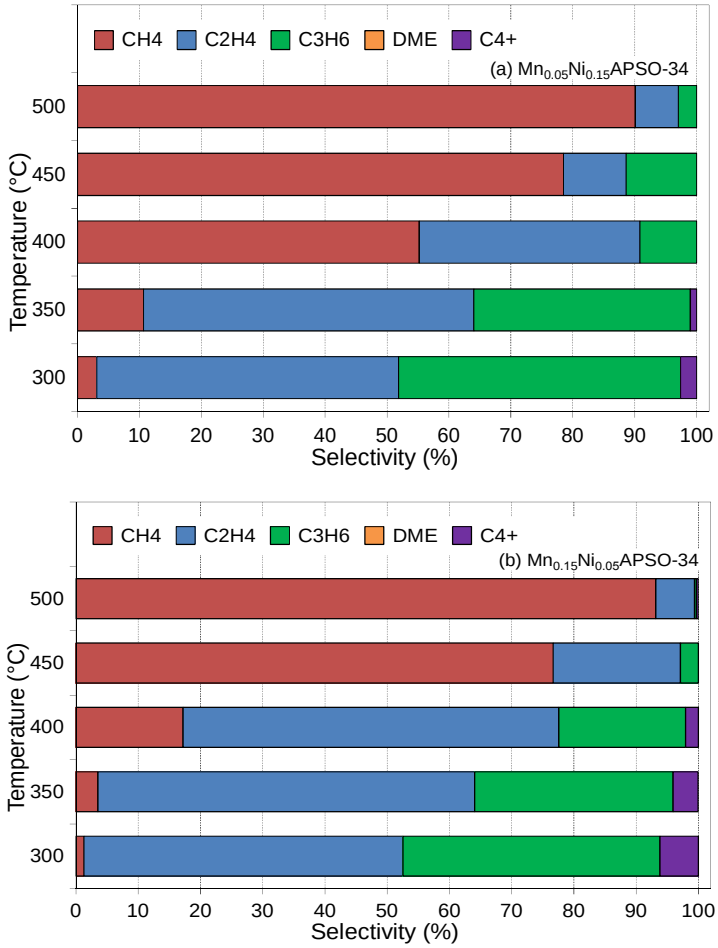

Fig. 10. Products selectivity over the synthesized nanostructured catalysts: (a) $Mn_{0.05}Ni_{0.15}$APSO-34 and (b) $Mn_{0.15}Ni_{0.05}$APSO-34

conversion to that observed for $Mn_{0.05}Ni_{0.15}$APSO-34 sample. $Mn_{0.15}Ni_{0.05}$APSO-34 nanostructured catalyst showed high selectivity towards ethylene and propylene; so, this nanostructured catalyst is deactivated slower than $Mn_{0.05}Ni_{0.15}$APSO-34. The effective TOS value for this nanostructured catalyst was about 3.5 h. The maximum selectivity of C_2-C_4 olefins was about 85% at 2h TOS. The DME in the product increased from 0.5% at 2 h to 60% at 5 h.

In the case of $Mn_{0.15}Ni_{0.05}$APSO-34 nanostructured catalyst, deactivation occurs slower than that of $Mn_{0.05}Ni_{0.15}$APSO-34. Particle size distribution and framework or extra-framework of metal ions may affect the nanostructured catalyst lifetime. The use of a nanostructured catalyst with uniform particle size at high concentrations of Mn enhances the accessibility of biomethanol into its cages resulting in a better catalytic performance. In comparison, high amount of DME in the products stream for $Mn_{0.05}Ni_{0.15}$APSO-34 nanostructured catalyst can be due to its non-uniform particle size distribution which is evident from the FESEM analysis and extra-framework of Nickel forming Co and H_2. The latter in turn undergoes reaction to form methane. It was concluded that $Mn_{0.15}Ni_{0.05}$APSO-34 nanostructured catalyst had the best performance and longer catalyst lifetime under the studied operational conditions, followed by the order $Mn_{0.15}Ni_{0.05}$APSO-34> $Mn_{0.05}Ni_{0.15}$APSO-34.

4. Conclusions

It was shown that concentration of different metal ions has a significant effect on physicochemical properties as well as the

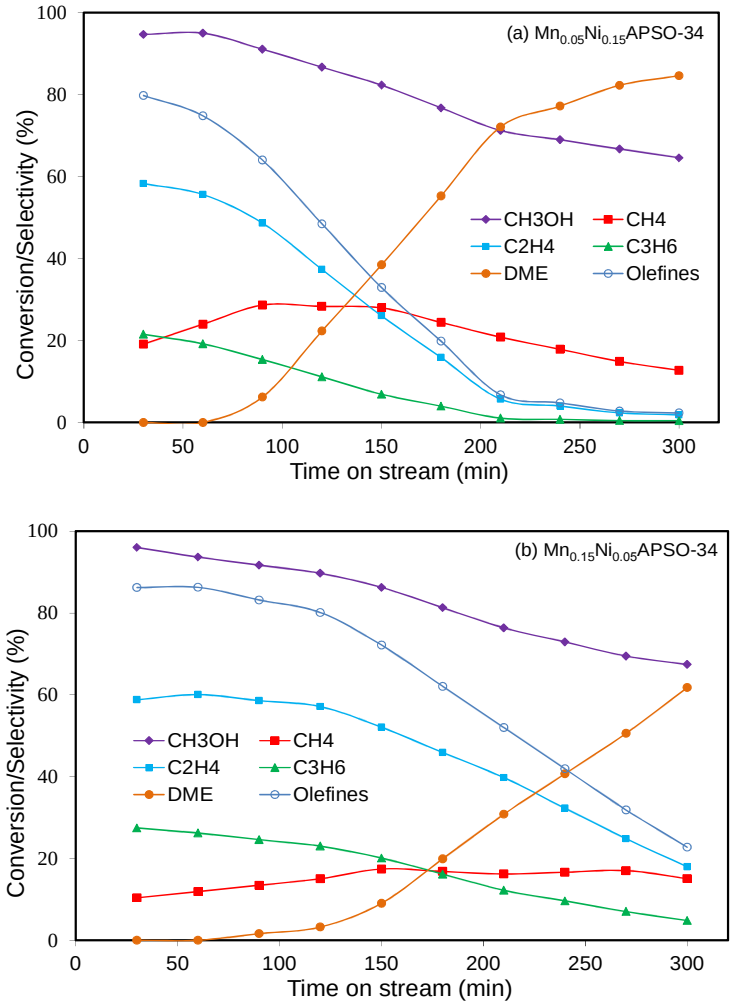

Fig. 11. Time on stream performance of synthesized nanostructured catalysts: (a) $Mn_{0.05}Ni_{0.15}$APSO-34 and (b) $Mn_{0.15}Ni_{0.05}$APSO-34

catalytic performance of MnNiAPSO-34 nanostructured catalyst in biomethanol to olefins conversion. According to the XRD patterns and FTIR analysis, $Mn_{0.05}Ni_{0.15}$APSO-34 and $Mn_{0.15}Ni_{0.05}$APSO-34 nanostructured catalysts have CHA structure attributed to SAPO-34 with 44.3 and 50.5 nm average crystallite sizes, respectively. FESEM images demonstrated that the particles have cubic shape structure for MnNiAPSO-34 nanostructured catalysts. The particle size of $Mn_{0.15}Ni_{0.05}$APSO-34 was larger than that of the $Mn_{0.05}Ni_{0.15}$APSO-34 nanostructured catalyst. It reveals that the incorporation of Mn metal ion, due to the increase in the particle growth, increases the particle size. The catalytic performance experiments showed that the conversion of biomethanol for the $Mn_{0.15}Ni_{0.05}$APSO-34 nanostructured catalyst with higher Mn content was similar to that for the $Mn_{0.05}Ni_{0.15}$APSO-34 sample. After incorporation of various concentrations of Ni^{2+} and Mn^{2+} cations into the framework, the $Mn_{0.15}Ni_{0.05}$APSO-34 nanostructured catalyst exhibited longer lifetime and higher selectivity to light olefins than the $Mn_{0.05}Ni_{0.15}$APSO-34 nanostructured catalyst.

Acknowledgements

The authors gratefully acknowledge Sahand University of Technology for the financial support of the research as well as Iran Nanotechnology Initiative Council for complementary financial supports.

References

1. D. Xiang, Y. Qian, Y. Man, S. Yang, "Techno-economic analysis of the coal-to-olefins process in comparison with the oil-to-olefins process", App. Energy, Vol. 113, 2014, pp. 639-647.
2. H. Nabil, H. Ismail, A.R. Azura, "Optimisation of accelerators and vulcanising systems on thermal stability of natural rubber/recycled ethylene–propylene–diene-monomer blends", Mater. Des., Vol. 53, 2014, pp. 651-661.
3. T. Alvaro-Munoz, C. Marquez-Alvarez, E. Sastre, "Use of different templates on SAPO-34 synthesis: Effect on the acidity and catalytic activity in the MTO reaction", Catal. Today, Vol. 179, 2012, pp. 27-34.
4. Y. K. Park, S. W. Baek, S. K. Ihm, "Effect of reaction conditions and catalytic properties on methanol conversion over SAPO-34", J. Ind. Eng. Chem., Vol. 7, 2001, pp. 167-172.
5. Z. Liu, C. Sun, G. Wang, Q. Wang, G. Cai, "New progress in R&D of lower olefin synthesis", Fuel Process. Technol., Vol. 62, 2000, pp. 161-172.
6. M. J. van Niekerk, J. C. Q. Fletcher, C. T. O'Connor, "Effect of catalyst modification on the conversion of methanol to light olefins over SAPO-34", Appl. Catal., A, Vol. 138, 1996, pp. 135-145.
7. C. Li, X. Yuan, K. Fujimoto, "Development of highly stable catalyst for methanol synthesis from carbon dioxide", Appl. Catal., A, Vol. 469, 2014, pp. 306-311.
8. A. García-Trenco, A. Martínez, "A simple and efficient approach to confine Cu/ZnO methanol synthesis catalysts in the ordered mesoporous SBA-15 silica", Catal. Today, Vol. 215, 2013, pp. 152-161.
9. Z. Chu, H. Chen, Y. Yu, Q. Wang, D. Fang, "Surfactant-assisted preparation of Cu/ZnO/Al2O3 catalyst for methanol synthesis from syngas", J. Mol. Catal. A: Chem., Vol. 366, 2013, pp. 48-53.
10. Y. Chen, Y. Wu, L. Tao, B. Dai, M. Yang, Z. Chen, X. Zhu, "Dehydration reaction of bio-ethanol to ethylene over modified SAPO catalysts", J. Ind. Eng. Chem., Vol. 16, 2010, pp. 717-722.
11. B. Vora, J.Q. Chen, A. Bozzano, B. Glover, P. Barger, "Various routes to methane utilization—SAPO-34 catalysis offers the best option", Catalysis today, Vol. 141, 2009, pp. 77-83.
12. M. S. Souza, E. C. G. Aguieiras, M. A. P. da Silva, M. A. P. Langone, "Biodiesel synthesis via esterification of feedstock with high content of free fatty acids", Applied biochemistry and biotechnology, Vol. 154, 2009, pp. 74-88.
13. S. Wang, L. Baxter, F. Fonseca, "Biomass fly ash in concrete: SEM, EDX and ESEM analysis", Fuel, Vol. 87, 2008, pp. 372-379.
14. T. Dogu, D. Varisli, "Alcohols as alternatives to petroleum for environmentally clean fuels and petrochemicals", Turkish Journal of Chemistry, Vol. 31, 2007, pp. 551.
15. V. Hulea, E. Huguet, C. Cammarano, A. Lacarriere, R. Durand, C. Leroi, R. Cadours, B. Coq, "Conversion of methyl mercaptan and methanol to hydrocarbons over solid acid catalysts – A comparative study", Appl. Catal., B, Vol. 144, 2014, pp. 547-553.
16. L. Wu, Z. Liu, L. Xia, M. Qiu, X. Liu, H. Zhu, Y. Sun, "Effect of SAPO-34 molecular sieve morphology on methanol to olefins performance", Chin. J. Catal., Vol. 34, 2013, pp. 1348-1356.
17. S. Tian, S. Ji, D. Lü, B. Bai, Q. Sun, "Preparation of modified Ce-SAPO-34 catalysts and their catalytic performances of methanol to olefins", J. Energy Chem., Vol. 22, 2013, pp. 605-609.
18. T. Álvaro-Muñoz, C. Márquez-Álvarez, E. Sastre, "Effect of silicon content on the catalytic behavior of chabazite type silicoaluminophosphate in the transformation of methanol to short chain olefins", Catal. Today, Vol. 213, 2013, pp. 219-225.
19. T. Álvaro-Muñoz, C. Márquez-Álvarez, E. Sastre, "Enhanced stability in the methanol-to-olefins process shown by SAPO-34 catalysts synthesized in biphasic medium", Catal. Today, Vol. 215, 2013, pp. 208-215.
20. D. Chen, K. Moljord, A. Holmen, "A Methanol to Olefins Review: Diffusion, Coke Formation and Deactivation on SAPO type catalysts", Microporous and mesoporous materials, Vol. 3, 2012,

pp. 23-39.
21. K. Y. Lee, H. J. Chae, S. Y. Jeong, G. Seo, "Effect of crystallite size of SAPO-34 catalysts on their induction period and deactivation in methanol-to-olefin reactions", Applied Catalysis A: General, Vol. 369, 2009, pp. 60-66.
22. A. Izadbakhsh, F. Farhadi, F. Khorasheh, S. Sahebdelfar, M. Asadi, Y.Z. Feng, "Effect of SAPO-34's composition on its physico-chemical properties and deactivation in MTO process", Appl. Catal., A, Vol. 364, 2009, pp. 48-56.
23. M. Stocker, "Methanol-to-hydrocarbons: catalytic materials and their behavior", Microporous Mesoporous Mater., Vol. 29, 1999, pp. 3-48.
24. M. Kang, "Methanol conversion on metal-incorporated SAPO-34s (MeAPSO-34s) ", J. Mol. Catal. A: Chem., Vol. 160, 2000, pp. 437-444.
25. F. C. Sena, B. F. de Souza, N. C. de Almeida, J.S. Cardoso, L.D. Fernandes, "Influence of framework composition over SAPO-34 and MeAPSO-34 acidity", Appl. Catal., A, Vol. 406, 2011, pp. 59-62.
26. N. Z. Rajic, "Open-framework aluminophosphates: synthesis, characterization and transition metal modifications", J. Serb. Chem. Soc., Vol. 70, 2005, pp. 371-391.
27. L. Xu, Z. Liu, A. Du, Y. Wei, Z. Sun, "Synthesis, characterization, and MTO performance of MeAPSO-34 molecular sieves", Studies in surface science and catalysis, Vol. 147, 2004, pp. 445-450.
28. M. Hartmann, L. Kevan, "Substitution of transition metal ions into aluminophosphates and silicoaluminophosphates: characterization and relation to catalysis", Res. Chem. Intermed., Vol. 28, 2002, pp. 625-695.
29. G. Back, Y. Kim, Y.S. Cho, Y.I. Lee, C.W. Lee, "Comparative Evaluation of Mn (II) Framework Substitution in MnAPSO-34 and Mn-Impregnated SAPO-34 Molecular Sieves Studied by Electron Spin Resonance and Electron Spin Echo Modulation Spectroscopy", Journal of the Korean Magnetic Resonance Society, Vol. 6, 2002, pp. 20-37.
30. M. Salmasi, S. Fatemi, A. Taheri Najafabadi, "Improvement of light olefins selectivity and catalyst lifetime in MTO reaction; using Ni and Mg-modified SAPO-34 synthesized by combination of two templates", J. Ind. Eng. Chem., Vol. 17, 2011, pp. 755-761.
31. D. R. Dubois, D. L. Obrzut, J. Liu, J. Thundimadathil, P. M. Adekkanattu, J. A. Guin, A. Punnoose, M.S. Seehra, "Conversion of methanol to olefins over cobalt-, manganese-and nickel-incorporated SAPO-34 molecular sieves", Fuel Process. Technol., Vol. 83, 2003, pp. 203-218.
32. M. Kang, C. T. Lee, "Synthesis of Ga-incorporated SAPO-34s (GaAPSO-34) and their catalytic performance on methanol conversion", J. Mol. Catal. A: Chem., Vol. 150, 1999, pp. 213-222.
33. D. Zhang, Y. Wei, L. Xu, F. Chang, Z. Liu, S. Meng, B.L. Su, Z. Liu, "MgAPSO-34 molecular sieves with various Mg stoichiometries: Synthesis, characterization and catalytic behavior in the direct transformation of chloromethane into light olefins", Microporous Mesoporous Mater., Vol. 116, 2008, pp. 684-692.
34. Y. Wei, Y. He, D. Zhang, L. Xu, S. Meng, Z. Liu, B.L. Su, "Study of Mn incorporation into SAPO framework: Synthesis, characterization and catalysis in chloromethane conversion to light olefins", Microporous Mesoporous Mater., Vol. 90, 2006, pp. 188-197.
35. M. Inoue, P. Dhupatemiya, S. Phatanasri, T. Inui, "Synthesis course of the Ni-SAPO-34 catalyst for methanol-to-olefin conversion", Microporous Mesoporous Mater., Vol. 28, 1999, pp. 19-24.
36. T. Inui, M. Kang, "Reliable procedure for the synthesis of Ni-SAPO-34 as a highly selective catalyst for methanol to ethylene conversion", Appl. Catal., A, Vol. 164, 1997, pp. 211-223.
37. S. Hotevar, J. Levec, "Acidity and catalytic activity of McAPSO-34 (Me = Co, Mn, Cr), SAPO-34, and H-ZSM-5 molecular sieves in methanol dehydration", J. Catal., Vol. 135, 1992, pp. 518-532.
38. F. Rahmani, M. Haghighi, P. Estifaee, "Synthesis and characterization of

Pt/Al2O3–CeO2 nanocatalyst used for toluene abatement from waste gas streams at low temperature: Conventional vs. plasma–ultrasound hybrid synthesis methods", Microporous Mesoporous Mater., Vol. 185, 2014, pp. 213-223.

39. S. Allahyari, M. Haghighi, A. Ebadi, S. Hosseinzadeh, "Ultrasound Assisted Co-Precipitation of Nanostructured CuO-ZnO-Al2O3 over HZSM-5: Effect of Precursor and Irradiation Power on Nanocatalyst Properties and Catalytic Performance for Direct Syngas to DME", Ultrason. Sonochem., Vol. 21, 2014, pp. 663-673.
40. S. Aghamohammadi, M. Haghighi, M. Charghand, "Methanol conversion to light olefins over nanostructured CeAPSO-34 catalyst: Thermodynamic analysis of overall reactions and effect of template type on catalytic properties and performance", Mater. Res. Bull., Vol. 50, 2014, pp. 462-475.
41. Y. Vafaeian, M. Haghighi, S. Aghamohammadi, "Ultrasound Assisted Dispersion of Different Amount of Ni over ZSM-5 Used as Nanostructured Catalyst for Hydrogen Production via CO2 Reforming of Methane", Energy Convers. Manage., Vol. 76, 2013, pp. 1093-1103.
42. S. M. Sajjadi, M. Haghighi, A. Alizadeh Eslami, F. Rahmani, "Hydrogen Production via CO2-Reforming of Methane over Cu and Co Doped Ni/Al2O3 Nanocatalyst: Impregnation vs. Sol-Gel Method and Effect of Process Conditions and Promoter", J Sol-Gel Sci Technol, Vol. 67, 2013, pp. 601-617.
43. N. Asgari, M. Haghighi, S. Shafiei, "Synthesis and Physicochemical Characterization of Nanostructured CeO2/Clinoptilolite for Catalytic Total Oxidation of Xylene at Low Temperature", Environ. Prog. Sustain. Energy., Vol. 32, 2013, pp. 587-597.
44. S. M. Alwahabi, G. F. Froment, "Single event kinetic modeling of the methanol-to-olefins process on SAPO-34", Ind. Eng. Chem. Res., Vol. 43, 2004, pp. 5098-5111.
45. A. T. Najafabadi, S. Fatemi, M. Sohrabi, M. Salmasi, "Kinetic modeling and optimization of the operating condition of MTO process on SAPO-34 catalyst", J. Ind. Eng. Chem., Vol. 4, 2011, pp. 43-58.
46. N. Fatourehchi, M. Sohrabi, S. J. Royaee, S. M. Mirarefin, "Preparation of SAPO-34 catalyst and presentation of a kinetic model for methanol to olefin process (MTO) ", Chem. Eng. Res. Des., Vol. 89, 2011, pp. 811-816.